

DESIGN OF A COMPACT INDUCTOR MATCHED TO A HOMOPOLAR GENERATOR

J. H. Gully, S. B. Pratap, M. S. Spann, W. F. Weldon, and H. H. Woodson
 Center for Electromechanics
 The University of Texas at Austin
 Austin, TX 78712

Summary

A liquid nitrogen pool-cooled, coaxial energy storage inductor is being designed and built to provide a load for a prototype compact homopolar generator (HPG). This is part of a continuing effort to produce a compact field-portable electromagnetic accelerator power supply.

Initial design parameters are that the coil store 3.1 MJ, representing a 50 percent transfer efficiency of energy stored in the HPG, with a transfer current of 1.0 MA. Coaxial conductor configurations are being investigated to eliminate high external magnetic fields, which have undesirable effects on nearby components. Also, coaxial inductors having a solid central conductor can withstand compressive magnetic loading at the inner radius of the material. This increases the achievable energy density, which is a function of the square of the magnetic flux density. The inductor will be made of aluminum and will be nested with the HPG in a low-resistance, compact configuration. Design and fabrication of the inductor are discussed.

Introduction

Since January 1980, The Center for Electromechanics at The University of Texas at Austin (CEM-UT), funded by the U.S. Army Armament Research and Development

Command (ARRADCOM) and the Defense Advanced Research Projects Agency (DARPA), has been developing the components of a high energy density, high current pulsed power supply to drive a field-portable electromagnetic (EM) railgun. The power supply being developed uses a homopolar generator as the primary energy store, an inductor for power conditioning, and an opening switch to divert the current into the railgun at the appropriate time (Fig. 1). Because the system is being developed to provide a technology base for a field-portable device, the primary constraints are that the power supply be compact and that it operate at high energy density.

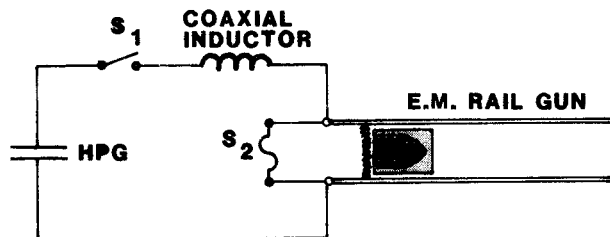


Fig. 1. EM railgun circuit with intermediate inductive energy store

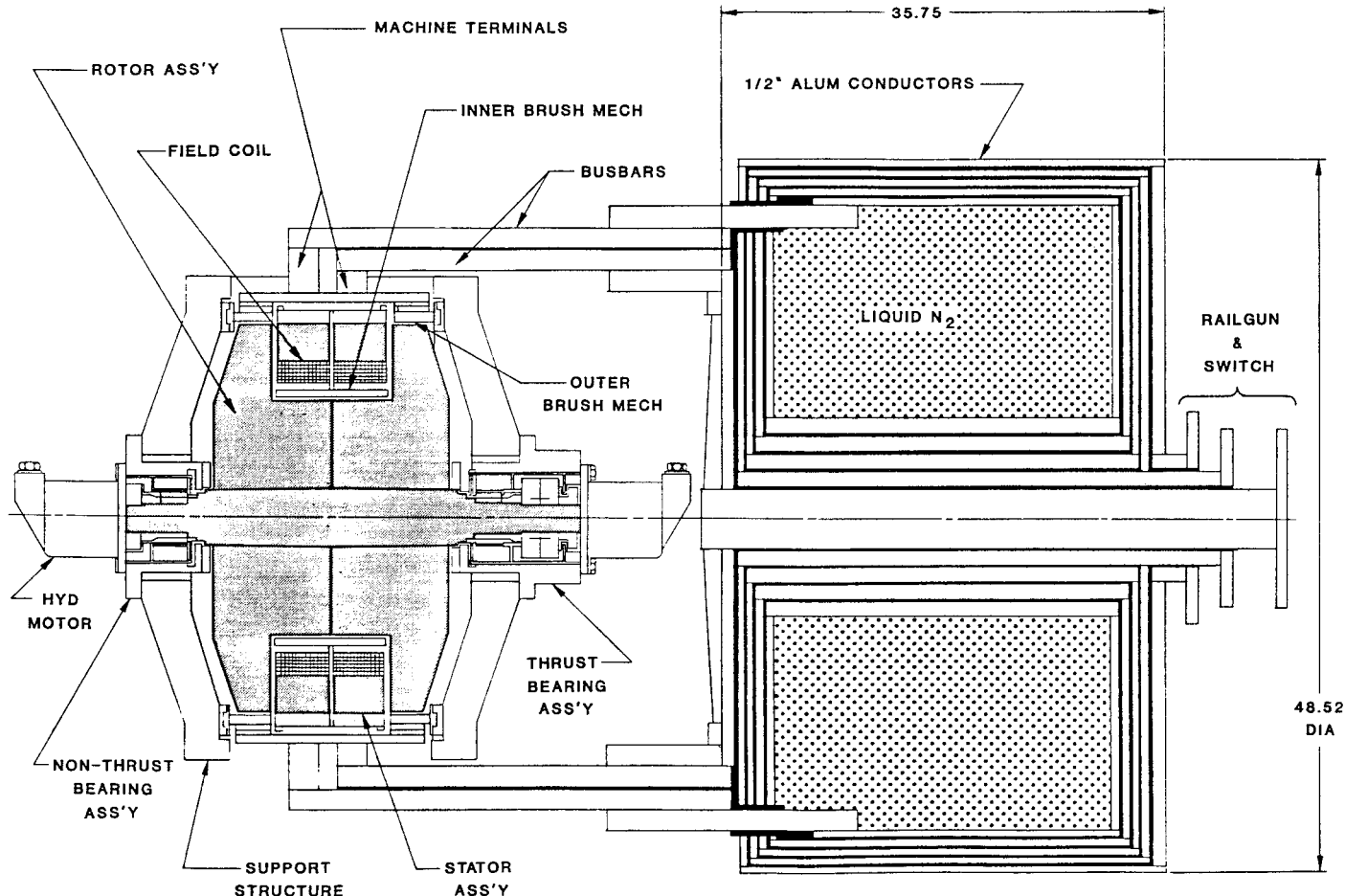


Fig. 2. Section through HPG and inductor

Report Documentation Page

*Form Approved
OMB No. 0704-0188*

Public reporting burden for the collection of information is estimated to average 1 hour per response, including the time for reviewing instructions, searching existing data sources, gathering and maintaining the data needed, and completing and reviewing the collection of information. Send comments regarding this burden estimate or any other aspect of this collection of information, including suggestions for reducing this burden, to Washington Headquarters Services, Directorate for Information Operations and Reports, 1215 Jefferson Davis Highway, Suite 1204, Arlington VA 22202-4302. Respondents should be aware that notwithstanding any other provision of law, no person shall be subject to a penalty for failing to comply with a collection of information if it does not display a currently valid OMB control number.

1. REPORT DATE JUN 1983	2. REPORT TYPE N/A	3. DATES COVERED -	
4. TITLE AND SUBTITLE Design Of A Compact Inductor Matched To A Homopolar Generator		5a. CONTRACT NUMBER	
		5b. GRANT NUMBER	
		5c. PROGRAM ELEMENT NUMBER	
6. AUTHOR(S)		5d. PROJECT NUMBER	
		5e. TASK NUMBER	
		5f. WORK UNIT NUMBER	
7. PERFORMING ORGANIZATION NAME(S) AND ADDRESS(ES) Center for Electromechanics The University of Texas at Austin Austin, TX 78712		8. PERFORMING ORGANIZATION REPORT NUMBER	
9. SPONSORING/MONITORING AGENCY NAME(S) AND ADDRESS(ES)		10. SPONSOR/MONITOR'S ACRONYM(S)	
		11. SPONSOR/MONITOR'S REPORT NUMBER(S)	
12. DISTRIBUTION/AVAILABILITY STATEMENT Approved for public release, distribution unlimited			
13. SUPPLEMENTARY NOTES See also ADM002371. 2013 IEEE Pulsed Power Conference, Digest of Technical Papers 1976-2013, and Abstracts of the 2013 IEEE International Conference on Plasma Science. Held in San Francisco, CA on 16-21 June 2013. U.S. Government or Federal Purpose Rights License.			
14. ABSTRACT			
15. SUBJECT TERMS			
16. SECURITY CLASSIFICATION OF:			17. LIMITATION OF ABSTRACT SAR
a. REPORT unclassified	b. ABSTRACT unclassified	c. THIS PAGE unclassified	
			18. NUMBER OF PAGES 4
			19a. NAME OF RESPONSIBLE PERSON

The initial step in developing the power supply was to design, fabricate, and test the primary energy store, an HPG designed to advance significantly the state of the art in terms of energy delivered and power generated per unit mass. This step was completed in August 1982 with the successful testing of a 3400-lb_m, 6.2-MJ, 5.4-kF machine that generated 1.02 MA.¹ The second phase of the program, now nearing completion, consists of upgrading the HPG and building a matched energy storage inductor (Fig. 2). This paper presents results of the parametric study to select a configuration, design, and fabrication technique, and calculated the performance of the energy storage inductor.

In an HPG-powered EM railgun circuit, the inductor acts as a pulse compression stage and also serves as a current source for the railgun, minimizing current droop as the back emf of the railgun rises. The inductor is charged in about 0.25 s by the HPG and is then discharged rapidly, in about 2 to 4 ms, into the railgun. Discharge is initiated when the current in the inductor peaks, at which time maximum energy has been transferred from the HPG.

To be consistent with the field portability requirement, the inductor must be lightweight and compact. This implies high magnetic fields, which result in high magnetic pressures on the conductors and insulation. Back emf of the railgun is anticipated to be about 1 kV. The insulation is therefore being designed to withstand 5 kV. Because of their detrimental effects on the performance of nearby components and because they represent a detectable EM signature, the high magnetic fields must be confined.

Design Parameters

The inductor baseline design called for a 50 percent transfer of energy, or 3.1 MJ, at 1 MA from the HPG. This current level was selected to test the capability of the 750-kA rated HPG and is at a level sufficient to allow an experimental investigation of armature reaction of the HPG.

Because of the low voltage characteristics of HPGs, the resistance of the coil during the charging process must be minimized. Initial studies showed material selection to be a major factor in optimization of the design. A study of the material options showed that liquid nitrogen (LN₂) cooled, high conductivity aluminum has about the same resistivity as LN₂-cooled copper, but has less than one-third its mass. At the charging frequency, cryogenically cooling the material results in an effective reduction of a factor of 4.2 below room temperature resistivity. Of the two readily available high conductivity aluminum alloys, types 6101 and 1100, only the 1100 series was available in the desired sizes. Therefore, the design was based upon a yield strength of 117 MN/m² (17 ksi) and a resistivity of $3.4 \times 10^{-9} \Omega\text{-m}$, the properties of half-hard 1100 series aluminum at LN₂ temperature.

For the purpose of analysis, the total inductance of the coil is broken into two components -- the inductances resulting from air-core flux linkages and the partial flux linkages in the conductors. In the theoretical case of an instantaneous discharge, magnetic diffusion effects result in the energy in the partial flux linkages (internal inductance) being trapped and dissipated in heating of the conductors rather than driving the railgun projectiles. For the rapid discharge into a railgun, about 4 ms, 70 percent of the energy stored in internal inductance is trapped. Therefore, the internal inductance must be minimized.

Candidate Configuration Comparison

Four inductor configurations were considered: the traditional Brooks coil and Bitter plate inductors and two new concepts, one with "pie-shaped" conductors and the other with coaxial conductors (Fig. 3).

The Brooks coil has a minimum mass for a given inductance. It produces high external magnetic fields, however, that must be contained within ferromagnetic shields. This adds substantial weight and volume, and renders this configuration unacceptable.

The toroidal Bitter plate inductor reduces the external magnetic fields, since the main magnetic field is confined to the core. A single-start inductor has a net magnetomotive force that produces an axial magnetic field. Also, a single-start configuration results in

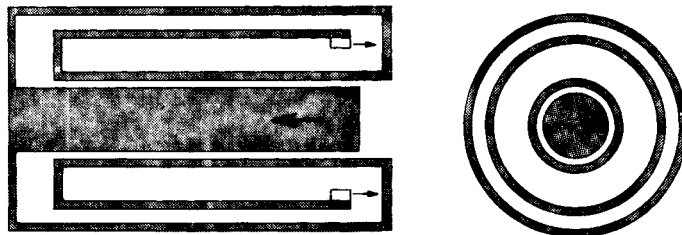


Fig. 3a. Coaxial inductor design

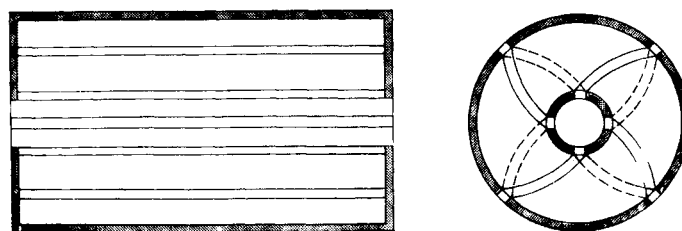


Fig. 3b. Pie-segment inductor design

an unacceptably high resistance or a complex busbar interface with the HPG. A four-start design eliminates the external field and results in an acceptable busbar network. Since the four-start design has its four segments in parallel, however, each segment must have four times the total inductance desired. This requires increasing the size and/or number of turns in each segment. The toroidal Bitter plate design is therefore either physically large, or it has an unacceptably high resistance.

The coaxial conductor design has a relatively good charging efficiency and fully compensates the magnetic field. Also, the design nests very well with the HPG, and since the inner coaxial conductors support each other in compressive loading, the high magnetic fields at the inner diameter are easily withstood. Since the cross section for current flow extends over the entire circumferential length of each turn, the skin depth limitation on the thickness is less of a problem. As the number of turns increases, however, the discharge efficiency decreases because of eddy currents generated in conductors by currents in adjacent conductors.

This "proximity effect" is reduced in the "pie-segment" conductor design because the coupling between adjacent conductors is minimized. Therefore, the pie-segment conductor design has a better discharge efficiency than the coaxial conductor design. It compensates the magnetic field almost as well as the coaxial design and withstands the magnetic pressures on the inner conductors similarly to the coaxial design. Its charging efficiency is lower because the circumferential conductor width available to carry current for each turn is reduced by the number of turns. Also, the pie-segment conductor design has a single start and thus does not interface well with the HPG output terminals.

Figure 4 is a graph of the available energy per unit system mass (HPG/busbar/inductor) vs the number of turns for the pie-segment and coaxial inductor configurations. Both inductors are assumed to be made of

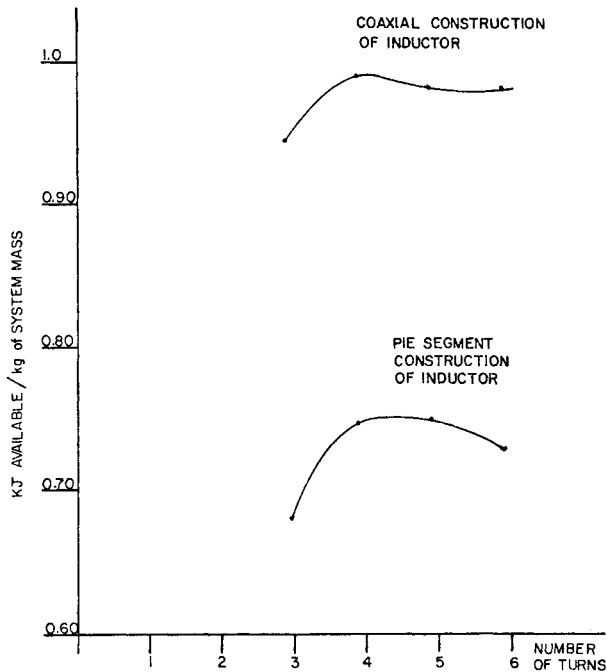


Fig. 4. System mass vs number of turns

the same material and store 3.1 MJ at 1.0 MA. From the figure it can be concluded that even though the coaxial conductor design has a lower discharge efficiency, its overall performance is superior to the pie-segment design.

Inductor Design

From Fig. 4, it can be seen that either a four- or a five-turn coil is optimum. Because it has a 25 percent smaller volume, the five-turn design was selected. Type 1100 aluminum alloy was selected as the material because at LN₂ temperature it has the lowest resistivity per unit mass among available materials. The skin depth for this alloy at the charging frequency of 0.93

Hz is 3 cm (1.2 in.). In order to minimize system mass, it is desirable that the thickness of all conductors be less than the skin depth. Therefore, all of the inner conductors are 2.5 cm thick except for the center post, which has a 5-cm radius for structural reasons. The outer conductors and end plates are all 1.26 cm thick except for the outer end plates, which are 2.22 cm thick for structural reasons.

The magnetic field and the resulting magnetic pressure are highest at the inner conductors and decrease with increasing radius. Inner coaxial conductors are compressed by the magnetic field, the load being taken by the solid central post. Outer coaxial conductors are loaded in tension, but the field is low at this larger radius, and the resulting stresses are acceptable. End plates experience the full pressure profile from a maximum of 2,200 psi at the inner radius to a minimum of 200 psi at the outer radius. Maximum deflection is at the mean radius and is predicted to be 0.53 mm. Regions of highest stress are at the corners where the inner end plate is welded to the largest inner coaxial conductor and at the inner radii of the outer end plates. To prevent failure, the outer end plates are being thickened and a large fillet is being welded into the inner joint.

The coil is permanently assembled sequentially from the inside out (see Fig. 5). The first step is to weld together the inner bucket, which consists of a 2.5-cm thick rolled outer cylinder, a 2.5-cm thick end plate and an inner cylinder. After welding this "cake-pan," or "bucket," shape, it is machined to final dimension. Then the inner end plate on the crossover end is welded to the inner cylinder at its inner diameter and to the second bucket at its outer diameter. Buckets and end plates are spaced 0.32 cm apart with NEMA type G-7 (fiberglass-reinforced silicone) spacers. The procedure is repeated until five turns have been welded together. At this point, the space between conductors will be filled by vacuum impregnation with epoxy. The entire structure will then be coated with thermal insulation. Liquid nitrogen will be fed into the coil through an access hole at the top.

Predicted Performance

Figure 4 indicates a fairly flat optimum energy density for the coaxial inductor at around four turns. Although the four-turn coil has the lowest system mass, a five-turn coil has a 25-percent smaller volume, and

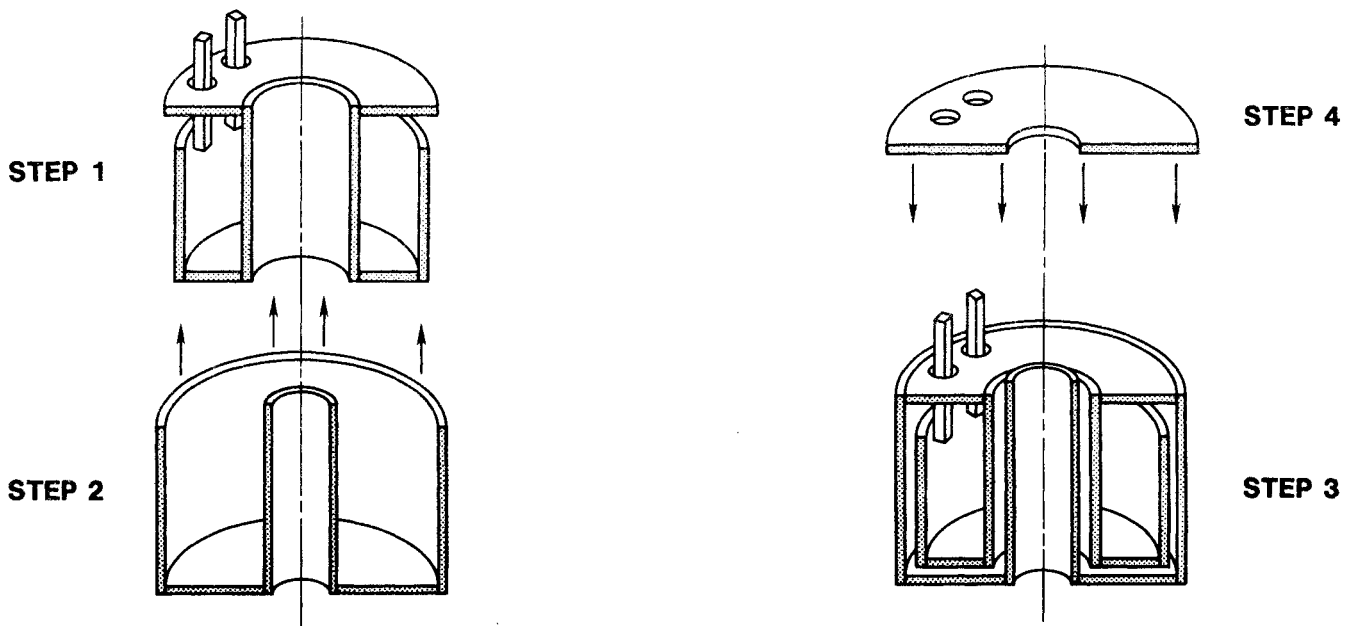


Fig. 5. Stages in assembly of coaxial inductor

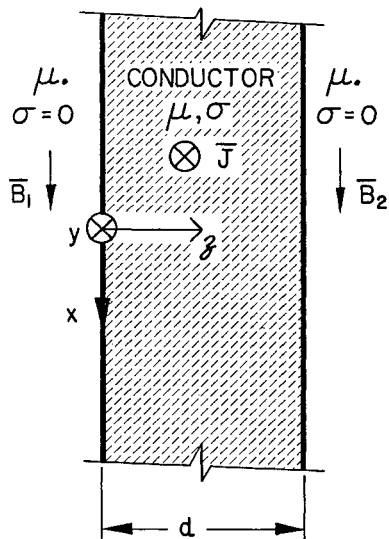
its weight penalty over a four-turn coil is small. A five-turn, 6.2- μ H at 1-MA coil was designed to store 3.1 MJ. Neglecting diffusion effects during charging, the governing equation is

$$I = \frac{V_0}{\omega_e L} \exp(-t/2\tau) \sin \omega_e t$$

- where
- I = current
 - V_0 = HPG open circuit voltage, including armature reaction
 - L = system inductance, $L_{HPG} + L_{Ind}$
 - C = capacitance
 - ω_e = electrical angular frequency, s^{-1}
 - $= \sqrt{1/(LC) - (1/(2\tau))^2}$
 - τ = time constant, L/R
 - t = time to current peak
 - $= \arctan(2L\omega_e/R)/\omega_e$
 - R = system resistance, $R_{HPG} + R_{Busbar} + R_{Ind}$.

To use this equation to evaluate the performance of the coil, electrical losses due to magnetic diffusion must be estimated. Losses in the conductors during charging were derived assuming steady-state ac conditions and a rectangular, rather than cylindrical, geometry. Figure 6 shows the system being analyzed, along with the variables.

Solving the magnetic diffusion equation in the frequency domain as a function of only the z-coordinates, the ratio of resistance at a particular frequency to the dc resistance is given by



\bar{B}_1, \bar{B}_2 = Magnetic flux densities at the boundary of the conductor
 μ = Magnetic permeability
 σ = Electrical conductivity

Fig. 6. A current carrying conductor with adjacent magnetic field

$$\frac{R}{R_0} = \frac{d}{\delta} \left\{ \frac{(B_2^2 + B_1^2)[e^{2d/\delta} - e^{-2d/\delta}] + 2\sin(2d/\delta)}{(B_2 - B_1)^2[(e^{d/\delta} - e^{-d/\delta})^2 \cos^2(d/\delta) + (e^{d/\delta} + e^{-d/\delta})^2 \sin^2(d/\delta)]} - \frac{4B_1 B_2 [e^{d/\delta} + e^{-d/\delta}] \sin d/\delta + (e^{d/\delta} - e^{-d/\delta}) \cos d/\delta}{(B_2 - B_1)^2[(e^{d/\delta} - e^{-d/\delta})^2 \cos^2(d/\delta) + (e^{d/\delta} + e^{-d/\delta})^2 \sin^2(d/\delta)]} \right\}$$

where $\delta = \text{skin depth}, \sqrt{2/(\omega\mu\sigma)}$.

Using this equation for the specific case of transferring 3.1 MJ at 1.0 MA, the dc resistive losses are 0.32 MJ, and the resistive losses including magnetic diffusion are 0.47 MJ, a 32-percent increase.

Losses during discharge, assuming an exponential decay are given by the expression

$$\Delta W_d = \frac{K_0^2}{\sigma d} \left[\frac{1}{2\alpha_d} + \sum_{n=1}^{\infty} \frac{\alpha_d^2 \tau_n^2}{\alpha_d \tau_n + 1} + 4(N^2 + N) \sum_{n_{\text{odd}}}^{\infty} \frac{\alpha_d^2 \tau_n^2}{\alpha_d \tau_n + 1} \right]$$

- where
- $\tau_n = \mu_0 \sigma d^2 / (\pi^2 n^2)$
 - N = number of conductors "outside of" the conductor under consideration
 - K_0 = peak surface current density, $I_{\text{peak}} / (2\pi r)$
 - α_d = inverse of discharge time constant

Figure 7 illustrates the discharge characteristics of the inductor. For very slow discharges, eddy currents are negligible, losses being predominantly those due to the dc resistance of the coil. Losses decrease with an increase in discharge rate because the dwell time of the current in the inductor decreases. As the discharge rate increases further, the eddy current losses increase to an instantaneous discharge asymptote when all of the internal energy is dissipated.

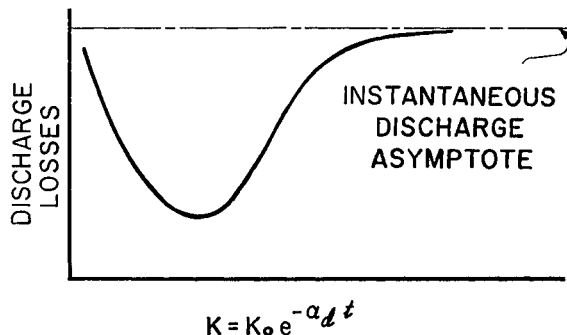


Fig. 7. Discharge losses

Conclusions

Fabrication of the inductor is scheduled to be completed during July 1983. Plans are to use the power supply to drive an 80-g tungsten projectile to 3 km/s. Based on test results, a second-generation high energy density HPG/inductor/opening switch power supply on a portable platform is planned. It is anticipated that the second-generation inductor will operate at higher energy density achieved by increasing the current density, number of turns, and stress levels.

References

1. Gully, J. H., et al., "Assembly and Testing of a Compact, Lightweight Homopolar Generator Power Supply," Proc. IEEE Intl. Pulsed Power Conf., 4th, Albuquerque, NM, June 6-8, 1983.